Received: 28 July 2023 | Accepted: 21 October 2023

DOI: 10.1002/jmv.29215

RESEARCH ARTICLE

JOURNAL OF MEDICAL VIROLOGY WILEY

Development of a rapid, sensitive detection method for SARS-CoV-2 and influenza virus based on recombinase polymerase amplification combined with CRISPR-Cas12a assay

Yuning Wang[1] | Liqiang Wu[1] | Xiaomei Yu[2] | Gang Wang[1] | Ting Pan[2] | Zhao Huang[2] | Ting Cui[2] | Tianxun Huang[1] | Zhentao Huang[1] | Libo Nie[2] | Chungen Qian[3]

[1]Department of Reagent Research and Development, Shenzhen YHLO Biotech Co., Ltd., Shenzhen, Guangdong, China

[2]Hunan Key Laboratory of Biomedical Nanomaterials and Devices, College of Life Science and Chemistry, Hunan University of Technology, Zhuzhou, Hunan, China

[3]Department of Biomedical Engineering, The Key Laboratory for Biomedical Photonics of MOE at Wuhan National Laboratory for Optoelectronics-Hubei Bioinformatics & Molecular Imaging Key Laboratory, Systems Biology Theme, Huazhong University of Science and Technology, Wuhan, Hubei, China

Correspondence

Chungen Qian, 1037 Luoyu Road, Hongshan District, Wuhan 430074, Hubei, China.
Email: chungen_qian@hust.edu.cn

Libo Nie, Postal Address: Taishan East Road, Tianyuan District, Zhuzhou 412007, Hunan, China.
Email: libonie@aliyun.com

Yuning Wang, Building 1, YHLO Biopark, Baolong 2nd Road, Baolong Subdistrict, Longgang District, Shenzhen 518115, Guangdong, China.
Email: yuningwang2010@aliyun.com

Abstract

Respiratory tract infections are associated with the most common diseases transmitted among people and remain a huge threat to global public health. Rapid and sensitive diagnosis of causative agents is critical for timely treatment and disease control. Here, we developed a novel method based on recombinase polymerase amplification (RPA) combined with CRISPR-Cas12a to detect three viral pathogens, including SARS-CoV-2, influenza A, and influenza B, which cause similar symptom complexes of flu cold in the respiratory tract. The detection method can be completed within 1 h, which is faster than other standard detection methods, and the limit of detection is approximately 10^2 copies/μL. Additionally, this detection system is highly specific and there is no cross-reactivity with other common respiratory tract pathogens. Based on this assay, we further developed a more simplified RPA/CRISPR-Cas12a system combined with lateral flow assay on a manual microfluidic chip, which can simultaneously detect these three viruses. This low-cost detection system is rapid and sensitive, which could be applied in the field and resource-limited areas without bulky and expensive instruments, providing powerful tools for the point-of-care diagnostic.

KEYWORDS

CRISPR-Cas12a, detection, influenza virus, microfluidic chip, RPA, SARS-CoV-2

1 | INTRODUCTION

Respiratory tract infections (RTIs) are one of the major causes of widespread diseases, especially leading to morbidity and mortality among children worldwide.[1,2] RTIs cause a series of upper and lower respiratory tract diseases ranging from the common cold to pneumonia.[3] Studies revealed the global death caused by acute respiratory infections is about 4 million per year, and pneumonia is the leading cause of death for children under 5 years old.[4,5] The causative agents are a collection of pathogens including viruses, bacteria, and mycoplasma,[6] while viral pathogens are one of the most common causes of respiratory infection.[7] Some viruses can cause highly contagious infections that continue spreading seasonally and may lead to death. For example, influenza (flu) is a communicable viral illness that affects the respiratory tract. Influenza-caused pneumonia was considered one of the top death

Yuning Wang and Liqiang Wu contributed equally to this work.

illnesses in many countries. It is especially risky for people with underlying diseases, which are very likely to develop complications after infection.[8,9] Influenza virus is comprised of segmented negative-sense single-stranded RNA genomes categorized into four genera from A, B, C, and D. Influenza A (H1N1, H3N2 subtypes) and B are the main causes of highly contiguous seasonal flu that occurs every year from the fall to early spring.[10,11] The Centers for Disease Control and Prevention estimates seasonal flu has resulted in 9–41 million cases and 14 000–52 000 deaths annually in the United States between 2010 and 2020.[8] The preliminary estimates of the 2022–2023 flu season have resulted in 27–54 million illnesses and 19 000–58 000 flu deaths.[9] Therefore, public issues caused by flu illness are serious such as hospitalization burden and productivity losses. Given these circumstances, early detection of the flu is crucial for controlling its spread and saving public resources.

A newly emerged coronavirus identified as severe acute respiratory syndrome coronavirus 2 (SARS-CoV-2) caused a large outbreak in 2019, then evoked a global pandemic known as COVID-19.[12,13] SARS-CoV-2 spread worldwide rapidly and caused about 6.8 million deaths worldwide, resulting in lockdowns in many countries to interrupt virus transmission.[14,15] It is well known that COVID-19 can be mild or severe, and has become one of the major public health threats in the world. SARS-CoV-2 is an RNA virus that primarily targets nasal ciliated cells and afterward, infection causes atypical pneumonia from mild to severe inspiratory symptoms, initially with fever, cough, headache, and sore throat, which is very similar to the common cold and pneumonia caused by influenza viruses.[16–18] Hospitalized COVID-19 patients with acute respiratory distress syndrome are very likely to have the leading risk of vascular permeability, organ failure, and consequently death.[19] Enhanced transmission of SARS-CoV-2 primarily occurs through respiratory droplets among human-to-human, even with a high risk at the beginning of infection.[20] Individuals who were infected still get reinfected with COVID-19 which also increases the spread of this disease. COVID-19 spread to nearly every corner of the world which plunged the world into chaos. Efficient diagnostics are vital for the control of the disease.

Both influenza and COVID-19 are public health challenges and have been the most common circulating illness. The symptoms of influenza and COVID-19 are very similar, which makes it difficult for clinical diagnosis.[21,22] Co-infection of these two virus are common and might be a higher risk for poor health individuals.[23] Given the contiguous nature of influenza and COVID-19, there is an overwhelming demand for rapid diagnosis to distinguish these causative agents and provide proper antiviral medication immediately. In addition, the isolation of the infected individuals could break the viral transmission in time. Continued surveillance of influenza viruses and the SARS-CoV-2 helps monitor virus mutations that have pandemic potential and guides the selection of flu candidate vaccine strain.[24] Moreover, the identification of viral and bacterial infections is also useful in avoiding unnecessary antibiotic treatment that may lead to drug resistance.[25]

The recommended standard method for pathogen diagnosis such as real-time PCR (polymerase chain reaction) is the most powerful tool for SARS-CoV-2 screening during the pandemic with its superior sensitivity and specificity. However, the application of real-time PCR typically requires professional personnel with sophisticated instruments in a high-standard lab environment, which is also considered time-consuming and remains suboptimal turnaround time.[26–28] Therefore, alternative rapid and suitable diagnostic techniques for point-of-care (POC) detection are actively pursued outside centralized laboratories and become a critical strategy for the management of pathogenic infection.[26] Recently, recombinase polymerase amplification (RPA) combined with CRISPR/Cas technology (Clustered Regularly Interspaced Short Palindromic Repeats; CRISPR-associated (Cas) proteins) approaches have gained attention for on-site diagnosis.[28–30] Herein, we present a rapid and sensitive method identifying SARS-CoV-2, influenza A, and influenza B, based on RPA/CRISPR-Cas12a assay. Furthermore, we developed a microfluidic chip to perform RPA/CRSPR-Cas12a coupled with lateral flow assay for potential applications in different scenarios (Figure 1). This new

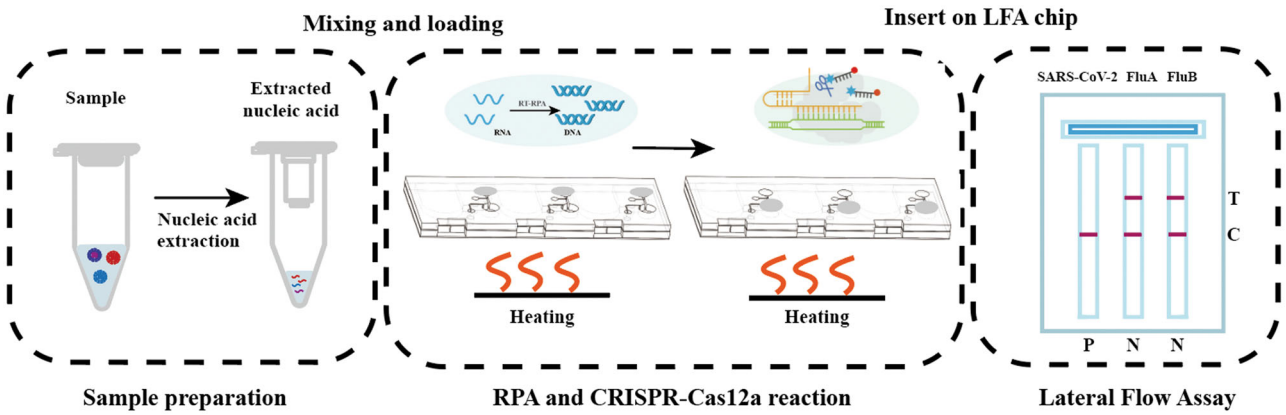

FIGURE 1 Workflow of RPA/CRISPR-Cas12a/lateral flow assay on the microfluidic chip as shown: Sample preparation, RPA amplification, CRISPR-Cas12a reaction, and lateral flow assay. C, control line; N, negative; P, positive; RPA, recombinase polymerase amplification; T, test line.

platform is rapid, sensitive, low-cost, and portable, which can be easily applied in circumstances with minimal resource settings as rare area clinical, community clinical facilities, and field conditions.

2 | MATERIALS AND METHODS

2.1 | Samples and reagents

SARS-CoV-2 pseudovirus with full-length nucleocapsid gene (N gene) was purchased from Yeasen Biotechnology Company. Inactivated influenza A, influenza B virus, and other viruses in cell cultures were purchased from Guangzhou BDS Biological Technology Company. The synthetic plasmid was made by pUC57 backbone with a synthesized target gene insertion. Viral genome was extracted following the extraction kit protocol (TaKaRa MiniBEST Viral RNA/DNA Extraction Kit Ver.5.0) from Takara Biomedical Technology Company and stored at −20°C for further assays. Oligos and CRISPR RNAs (crRNA) were synthesized by General Biol Company.

TwistAmp Basic RPA reagents were purchased from TwistDx. SuperScript IV Reverse Transcriptase was purchased from Invitrogen (Thermo Fisher). RNase H and EnGen Lba Cas12a (Cpf1) were purchased from New England Biolabs. Fluorescent dye SYBR I was purchased from Solarbio.

2.2 | RNA quantification

The DNA concentration (ng/μL) of synthesized plasmids containing target genes was measured by Qubit 4 Fluorometer and copy numbers were calculated according to the formula as follows: Concentration (copies/μL) = [DNA concentration (ng/μL) × 6.02 × 10^{23}/(length in nucleotides × 10^{9} × 650)]. These synthesized plasmids were serially diluted by a 10-fold ratio as DNA standards. As far as the extracted viral RNAs, a reverse-transcription PCR was performed with specific primers to reverse-transcribe RNA to complementary DNA (cDNA). Then a quantitative real-time PCR was performed to generate a standard curve formula with diluted plasmids, as well as cDNA samples. Finally, RNA concentration was calculated according to its Ct value and the standard curve formula.

2.3 | Reverse transcription-RPA (RT-RPA) procedure

All RT-RPA reactions were performed using TwistAmp Basic RPA reagent with SuperScript IV reverse transcriptase.[31] Each 25 μL reaction was conducted in two steps. First, a reaction mix was prepared containing 480 nM forward and reverse primer, 1.8 mM dNTPs, 12.5 μL 2× Reaction Buffer, 2.5 μL 10× Basic E-mix, 1.25 μL 20× Core Reaction Mix, 0.5 μL SuperScript IV reverse transcriptase, 1 μL RNase H and adjusted nuclease-free water (to 21.25 μL). After mixing, the reagents were aliquoted into PCR tubes. Then 2.5 μL template was added into the reagents and 1.25 μL of 280 mM magnesium acetate was added to the top of the reaction tube lid. The reagents were mixed thoroughly after spinning down the magnesium acetate droplets from the lids. The tubes were placed at 40°C on a metal bath quickly and incubated for 30 min. The products were saved for further CRISPR reaction.

2.4 | CRISPR reaction

A total of 5 μL of RPA product was added to a 25 μL CRISPR system containing 75 nM crRNA, 75 nM Cas12a, 500 nM ss-DNA-FQ reporter (for fluorescence detection) or 10 nM ss-DNA-FB reporter (for lateral flow assay), and 2.5 μL NEB Buffer 2.1. The reagents were mixed and incubated at 37°C on a metal bath for 15 min. The fluorescence signal could be detected under the blue light system with the Tanon Mini Space 2000 machine. For lateral flow assay, 5 μL of CRISPR reaction products was diluted with 45 μL ddH_2O. Finally, the dilution was loaded on the sample pad area in the strip, and the results were observed after 5 min.

2.5 | Lateral flow strip

Gold nanoparticles (AuNPs) (0.01%) were conjugated with anti-FITC antibody under proper pH and then concentrated. Glass cellulose and sample pad were pretreated with buffer [0.01 M Tris-HCl (pH 7.4), 0.5% (wt/vol) PEG10000, 5% Trehalose, 0.5% (vol/vol) Triton X-100, 0.5% (wt/vol) Casein for glass cellulose; 0.01 M Tris-HCl (pH 7.4), 0.5% (wt/vol) Casein, 0.5% (vol/vol) Triton X-100, 0.5% (wt/vol) Trehalose for sample pad] and dried out at 50°C. AuNPs were sprayed on glass cellulose with proper concentrations. Streptavidin (1 mg/mL) was sprayed as a test line on the nitrocellulose membrane, while Goat anti-rabbit immunoglobulin G (IgG) (1mg/mL) was sprayed as a control line on the nitrocellulose membrane next to the test line. The nitrocellulose membrane was placed at 37°C overnight to dry out. The strips were assembled as shown in Figure 5A and were cut with 3.5 mm width. Paper strips were stored in a dry bag for further assays.

2.6 | Microfluidic chip design

The microfluidic chips were designed using AutoCAD software (Autodesk) (Figure 7A). The microfluidics chips consist of three parts, including the insertion chip, the reaction chip, and the lateral flow assay chip (LFA chip). Each part is assembled with various layers of PMMA (polymethyl methacrylate) chips. The three-dimensional geometry was created in SolidWorks to illustrate chip structure (Figure 7C,D).

PMMA chips were fabricated by Universal Laser Systems VLS3.50 machine, and engraved following the manufacturer's manual

with proper modifications. The cover layer was 0.3 mm PMMA and engraved with 10% speed and 100% efficiency. For the other layers, 2 mm PMMA was engraved with 5% speed and 100% efficiency. The reaction layer, buffer layer from the reaction chip, and strip layer from the LFA chip were stuck with transparent tape on both sides. For the reaction chip and the LFA chip, each layer was bound together and pressed at high temperature of vacuum hot pressing. The complete chip was finally assembled as shown in Figure 7B.

3 | RESULTS

3.1 | Development and screening of RT-RPA primers

The targets for primer design were selected based on the highly specific and conserved genes of each virus (Figure 2A). In this assay, the N gene segment was selected as the SARS-CoV-2 detection target, while the matrix (M) gene segment was selected for influenza A, and the nonstructural (NS) gene segment for influenza B.[32,33] Primers for each pathogen detection system were designed following the guidelines of the manufacturer (http://www.twistdx.co.uk/), avoiding homologous regions among closed species. Primers were blasted on the NCBI Primer-blast website for specificity. RPA can be performed on a real-time PCR machine if a DNA dye is added to the reaction.[34] To perform preliminary screening, we monitored amplification curves by adding SYBR Green fluorescent dye and RNA template into the RT-RPA reagent system on a quantification PCR machine, then primer combinations with highly efficient amplification and strong signal intensity were selected according to the condition of exponential curve among gradient targets. Further, we analyzed amplification products with DNA electrophoresis for the selected primer combinations. The results showed that the product matched the expected size as previously designed between 100 and 280 bp (Figure 2B). Therefore, the indicated primer combinations were confirmed and selected for further tests (Table S1).

3.2 | CRISPR system development and optimization

Cas12a protein is an RNA-guided DNA endonuclease that cleaves double-stranded DNA. More interestingly, it also nonspecifically cleaves single-stranded DNA when an activated ternary duplex is formed. Therefore, we synthesized a FAM fluorescence and a quencher labeled single-strand DNA (ss-DNA-FQ) as a reporter in the CRISPR system, which facilitated visualization of the readout due to the collateral cleavage of its target. This collateral cleavage activity can only be activated when the crRNA, Cas12a, and target DNA form a ternary complex. Thus, the Cas protein cleavages the ss-DNA-FQ reporter to generate a fluorescence signal that could be detected using the illuminator system (Figure 3A).

To achieve satisfactory performance, we optimized the work concentration of Cas12a and crRNA in the CRISPR system with SARS-CoV-2 as an example. First, we tested the working concentration of Cas12a from 0 to 100 nM. The results showed that 75 nM of Cas12a is the minimal optimal concentration (Figure 3B, left), which achieved the saturated intensity even with low yield RPA products input (Figure 3B, right). Next, we determined the optimal crRNA concentration from 0 to 100 nM, and the results showed that relatively high signal intensity was observed with crRNA concentration above 75 nM (Figure 3C). Together, we concluded that the

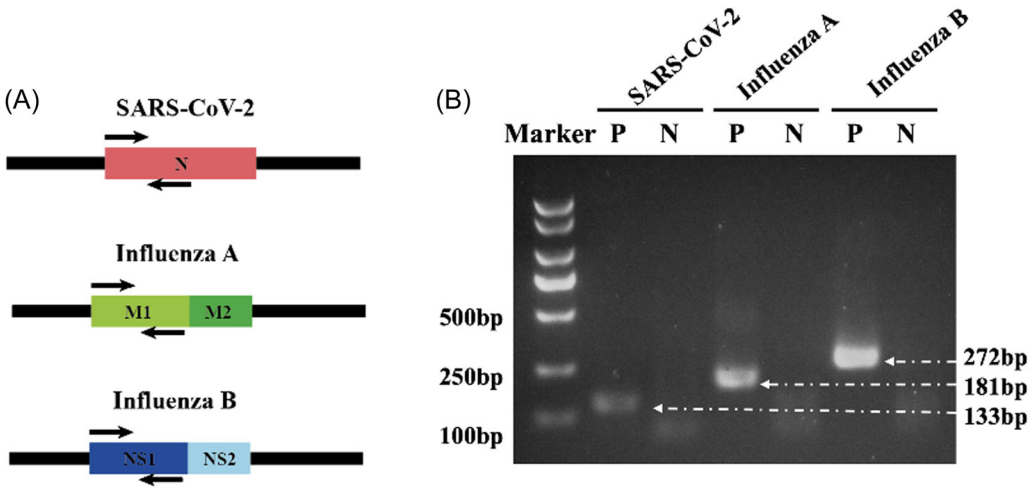

FIGURE 2 Primer design and confirmation. (A) Target selection and primer design: N gene for SARS-CoV-2, M gene for Influenza A, and NS gene for Influenza B. (B) Product confirmation by DNA electrophoresis. RPA was performed and the purified products were photographed under UV light. N, negative; P, positive; SARS-CoV-2, severe acute respiratory syndrome coronavirus 2.

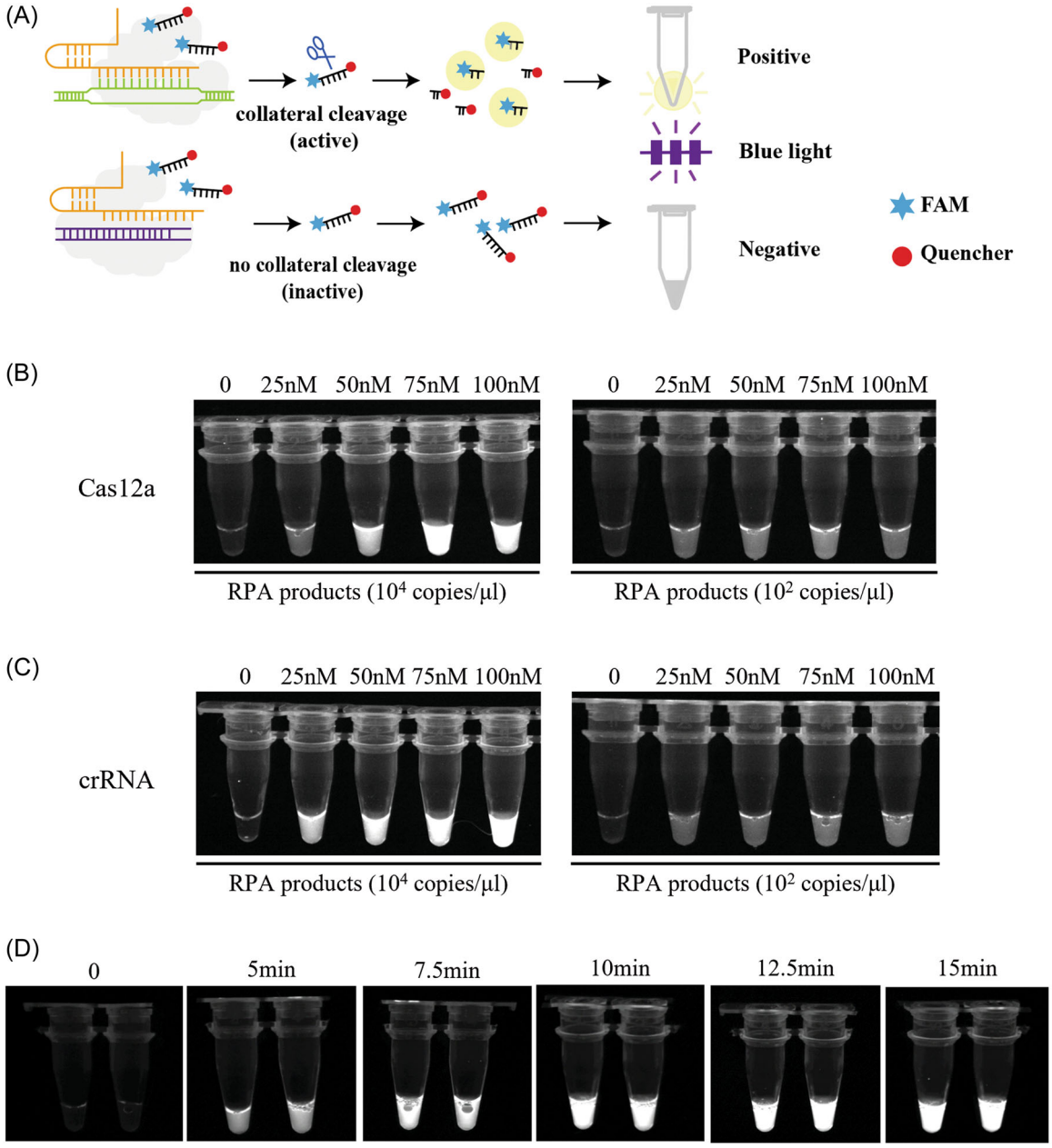

FIGURE 3 Schematic of CRISPR-Cas12a reaction and CRISPR system optimization. (A) Principle of CRISPR-12a fluorescence assay. Top: Presence of targets. Bottom: Absence of targets. (B) Optimal Cas12a working concentration from 0 to 100 nM as shown. RPA products of 10^4 copies/μL (left) or 10^2 copies/μL (right) input were detected as templates. (C) Optimal crRNA working concentration from 0 to 100 nM as shown. RPA products of 10^4 copies/μL (left) or 10^2 copies/μL (right) input were detected as templates. (D) Optimized minimal time of complete CRISPR reaction, and tubes were photographed for the indicated time after incubation. Duplicates were included for each time point. All photographs were taken under a blue light system. RPA, recombinase polymerase amplification.

optimal working concentration was 75 nM for crRNA and 75 nM for Cas12a. Furthermore, we detected the minimum working time for the CRISPR system. The fluorescence was scanned after 5 min of reaction, and the signals were collected every 2.5 min (Figure 3D). Fluorescence started to show up with a relatively weak intensity and achieved a saturated level in 10 min, indicating that 10 min is the minimal working time for complete cleavage in the CRISPR assay. For the following assays, we conduct a 15-min CRISPR reaction to achieve a complete reaction under different conditions.

3.3 | Detection limits of RPA/CRISPR-12a fluorescence detection assay

After primer sets and working parameters of the CRISPR system were confirmed, the detection limit of RPA/CRISPR-Cas12a fluorescence assay (RPA/CRISPR-Cas12a/Fluro) was investigated. First, all the viral RNA samples were quantified and diluted by a 10-fold ratio. We next determined the sensitivity of RPA/CRISPR-Cas12a under blue light with serial diluted RNA as templates. After incubation, all

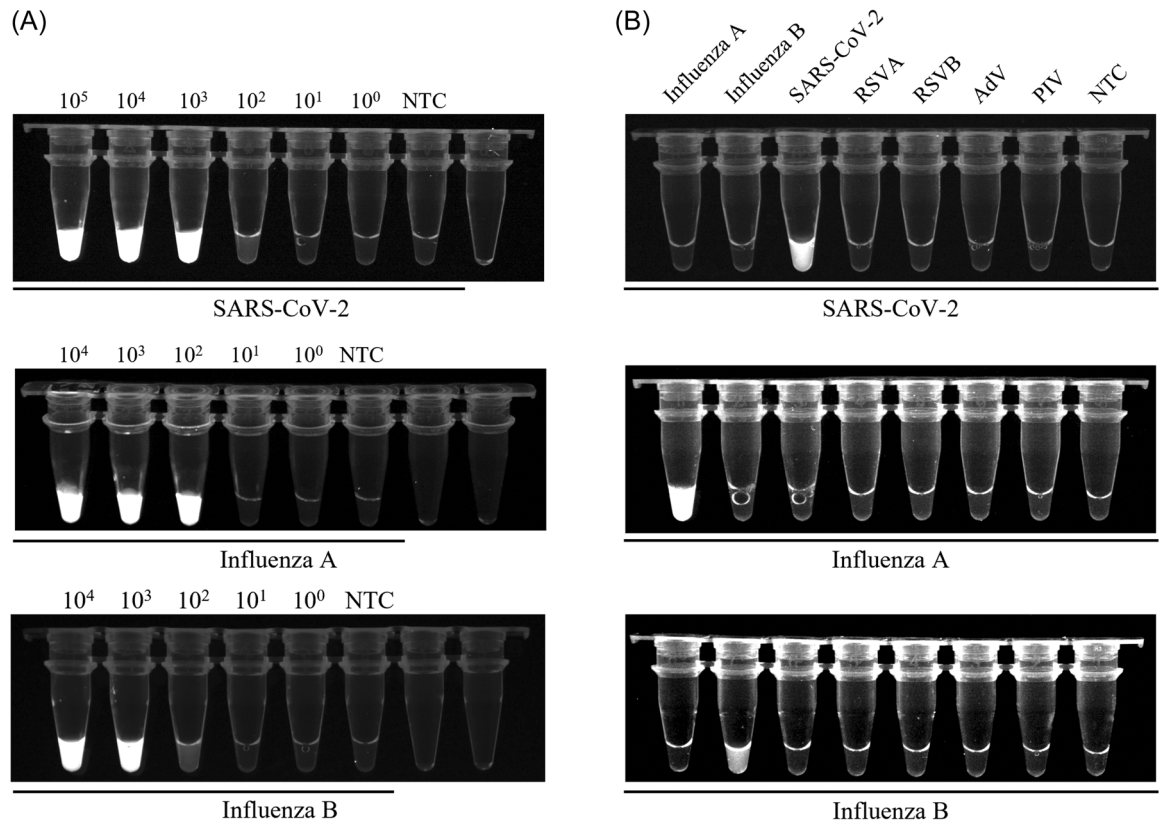

FIGURE 4 Detection limits and cross-reactivity evaluation of RPA/CRISPR-Cas12a/Fluro detection. (A) Detection limit evaluation. RNA samples from SARS-CoV-2 (top) were set from 10^5 copies/μL to 10^0 copy/μL, while RNA samples from influenza A (middle) or influenza B (bottom) were set from 10^4 copies/μL to 10^0 copy/μL. (B) Cross-reactivity evaluation of SARS-CoV-2, influenza A, and influenza B. The used templates in the array were influenza A, influenza B, SARS-CoV-2 pseudovirus, respiratory syncytial virus A (labeled as RSVA), respiratory syncytial virus B (labeled as RSVB), adenovirus (labeled as AdV), parainfluenza virus (labeled as PIV) or NTC (No template control). All tubes were photographed under a blue light system. SARS-CoV-2, severe acute respiratory syndrome coronavirus 2.

tubes were photographed. As results shown in Figure 4A, we observed the bright tube even with a low fluorescence intensity assumed as a positive reaction. For the limit of SARS-CoV-2 detection, we tested pseudovirus RNA samples with concentrations from 10^5 copies/μL to 1 copy/μL, and the fluorescence decreased to a relatively weak level at 10^2 copies/μL. For influenza A and influenza B detection, we tested RNA samples with concentrations from 10^4 copies/μL to 1 copy/μL. The signal for influenza A became weak at 10^2 copies/μL, while the signal was undetectable if below 10^2 copies/μL. The saturated signal for influenza B was observed at 10^4–10^2 copies/μL, while undetectable lower than 10^2 copies/μL. These results demonstrated that the detection limit is 10^2 copies/μL of RNA for SARS-CoV-2, influenza A, and influenza B, respectively.

3.4 | Cross-reactivity evaluation of the proposed method

A variety of respiratory pathogens can cause similar symptoms in the respiratory tract. Patients with diseases such as the common cold, influenza, and respiratory distress syndromes, are left with the challenge of defining infection agents that may cause cross infections.[35] To study the specificity of our detection system, we evaluated the interference between the target pathogen and other non-target respiratory viruses. The genomes of influenza A, influenza B, SARS-CoV-2 pseudovirus, respiratory syncytial virus A, respiratory syncytial virus B, Adenovirus, and parainfluenza viruses (I, II, III, and IV) were isolated as templates for each viral detection. The results demonstrated that only the indicated targets showed a bright signal under blue light (Figure 4B), suggesting there was no cross-reaction with other respiratory tract viral pathogens in these detections.

3.5 | Evaluation of RPA/CRISPR-Cas12a combined with lateral flow assay

In our assay, the RPA/CRISPR-Cas12a fluorescence detection system requires an illuminator image system that may restrict its portable utilization. To further simplify the described viral detection system, we developed a more usable platform using lateral flow assay (RPA/CRISPR-Cas12a/LFA), which could accomplish its POC application with minimal

instruments for the entire process, especially the final result readout. Paper-based lateral flow assay is an easy tool that simplifies nucleic acid detection at a low cost. In this assay, a reporter was used in the CRISPR system that labeled FAM on the 5′ end and biotin on the 3′ end. Gold nanoparticle conjugated with anti-FITC antibody in the conjugated pad was used to capture FAM reporter. Meanwhile, streptavidin (SA) and goat anti-rabbit IgG were immobilized on the test line and control line, respectively (Figure 5A). With the presence of targets, collateral cleavage of Cas enzyme is activated and results in cutting off reporters. And the reporters remain intact without the presence of the target. Only when the reporter is been cut off, AuNPs cannot be immobilized on the test line, so the test line is non-colored. Otherwise, AuNPs conjugate reporters then form a complex that is captured at the T line. Thus, both the T line and C line show up under the absence of target (Figure 5B).

We conducted assays with optimal concentrations of Cas12a and crRNA as described above, as well as a proper concentration of ssDNA-FB reporter to achieve the best detection performance, which shows clear evaluation criteria on strips as a positive or negative reaction. By a 10-fold dilution of RPA/CRISPR-Cas12a products, the lateral flow strip showed a clear readout for either the positive or negative test. Next, we evaluated the detection limit of RPA/CRISPR-Cas12a combined with lateral flow assay (Figure 6A). For SARS-CoV-2, the T line did not color as non-template test from 10^5–10^2 copies/μL RNA input test, which indicated that 10^2 copies/μL of RNA was the limit of detection. The test line was shown clearly when the input yield was less than 10^2 copies/μL. For influenza A, the test lines appeared at 10^2 RNA copies/μL with a faint color, which indicated a positive reaction. For input numbers less than 10^2 copies/μL, the test lines were clearly shown. For influenza B, there was no test line at 10^4–10^2 copies/μL RNA input but a clear line lower than 10^2 copies/μL RNA input number. Altogether, the detection limits of SARS-CoV-2, influenza A, and influenza B are 10^2 copies/μL, respectively.

In our evaluation, the detection limits of RPA/CRISPR-Cas12a coupled with lateral flow assay are consistent with RPA/CRISPR-12a fluorescence detection evaluated above. Additionally, the specificity test for lateral flow assay was investigated and there was no cross-reaction among those viruses (Figure 6B).

3.6 | On-chip testing

To reduce the workload of RPA/CRISPR-Cas12a/LFA which included several steps such as transferring, and diluting, a microfluidic chipset was designed that allows these three viruses detection to react separately and simultaneously in a closed reservoir, which could also reduce cross-contamination generated by opening tubes. This

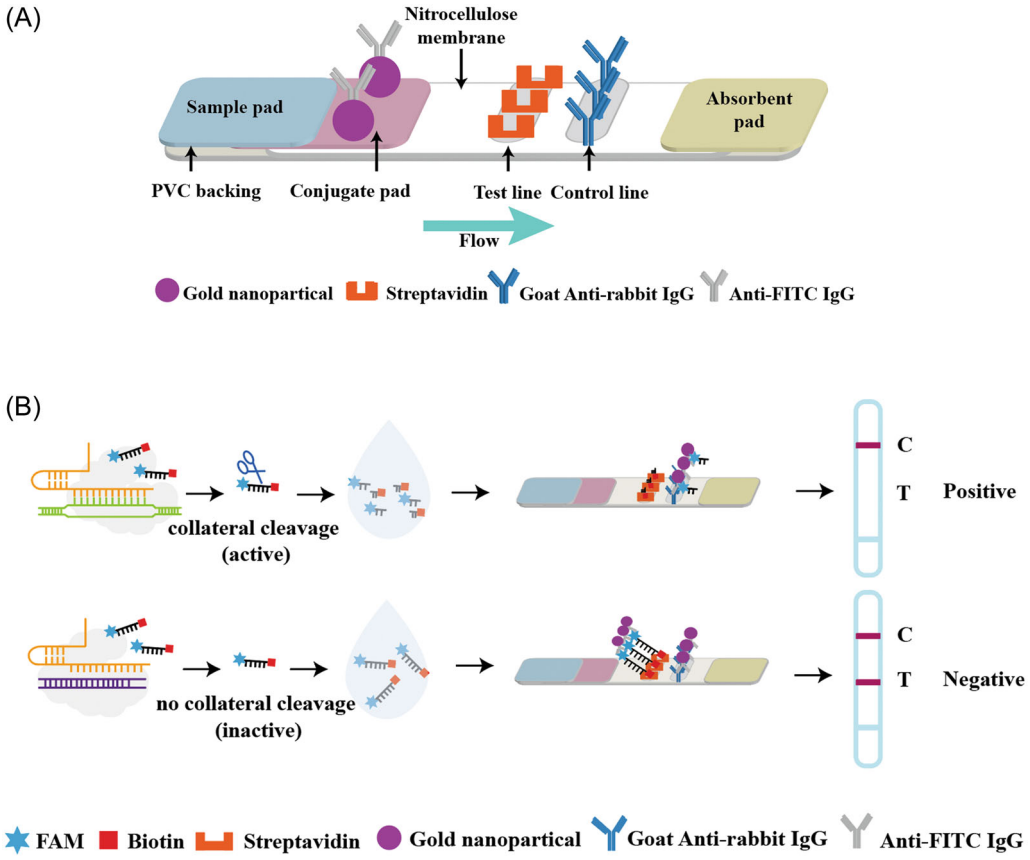

FIGURE 5 Schematic of CRISPR-Cas12a coupled with lateral flow assay. (A) Assembly of lateral flow strip. (B) Principle of RPA/CRISPR-Cas12a/LFA. The strip shows only the C line in the presence of targets indicated positive (top), and the strip shows both T and C lines without targets indicated negative (bottom). RPA, recombinase polymerase amplification.

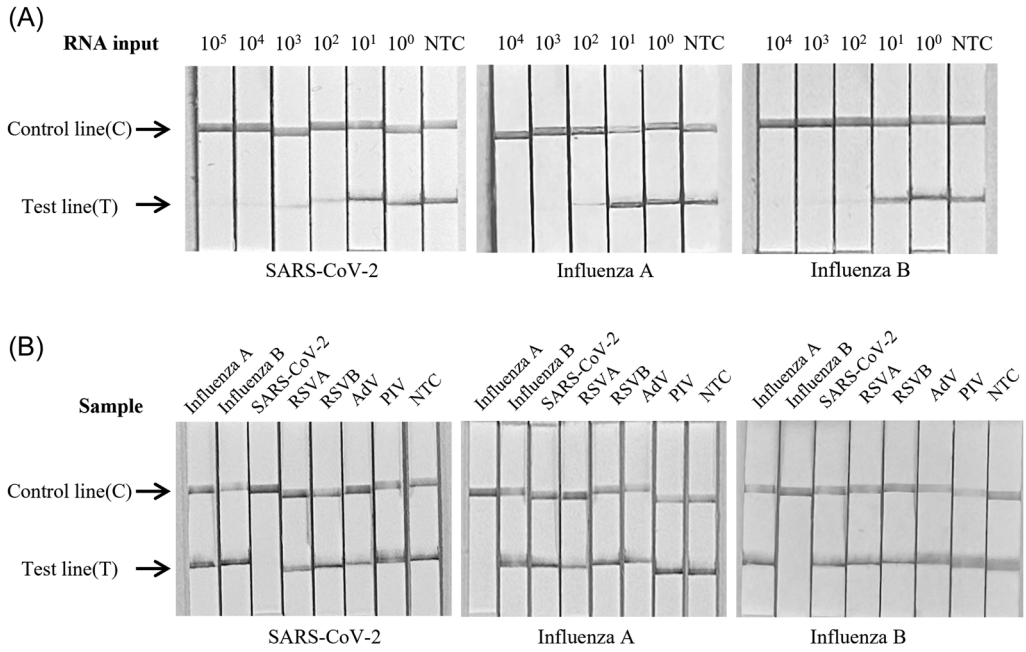

FIGURE 6 Detection limit and cross-reactivity evaluation of RPA/CRISPR-Cas12/LFA. (A) Detection limit evaluation. RNA samples from SARS-CoV-2 (left) were set from 10^5 copies/μL to 10^0 copy/μL, while RNA samples from influenza A (middle) or influenza B (right) were set from 10^4 copies/μL to 10^0 copy/μL. (B) Cross-reactivity evaluation. The templates in this array were influenza A, influenza B, SARS-CoV-2 pseudovirus, respiratory syncytial virus A (labeled as RSVA), respiratory syncytial virus B (labeled as RSVB), adenovirus (labeled as AdV), parainfluenza virus (labeled as PIV) or NTC. RPA, recombinase polymerase amplification.

microfluidic chip is assembled with three parts that are the reaction chip, the lateral flow assay chip (LFA chip), and the insertion chip, respectively (Figure 7A,B).

RPA reactions and CRISPR reactions were amplified on the five-layer reaction chip (Figure 7C). For on-chip testing, we slightly adjusted the reaction system volume. The RPA system was piped into the RPA chamber (~10 μL) through the sample inlet and this chamber was sealed with film. After incubation, the reaction reagents were gently manipulated to flow into the next larger CRISPR chamber (~30 μL) by tapping the chip in a vertical direction. RPA systems flowed into the CRISPR chamber through the 1.0 mm width channel, then CRISPR reagents were added to RPA products through a sample inlet. After 15 min of incubation, the chipset was assembled by inserting the reaction chip into the LFA chip vertically. All the incubations were performed on a metal bath. LFA chip was a three-layer chip embedded with three lateral flow strips separately (Figure 7D). A total of 300 μL ddH_2O was added into the dilution chamber. The insertion chip was loaded and pressed into the chamber slowly. Then the dilution fluid was pressed into the CRISPR chamber through the junction chamber in the connection layer first and afterward, the dilution fluid flowed to the dilution outlet eventually (Figure 8A,B). By this connection layer, multiple processes were separated from different spaces. The dilution fluid went up to the reaction layer and went down to the dilution layer smoothly through this layer. Finally, the CRISPR reaction system was diluted and pressed into the dilution outlet chamber adjacent to the strip chamber. The microfluidic chip was completely manually operated without the requirement of a complicated fluid power system. Using the insertion chip, the dilution fluid achieved flowability through multiple layers.

4 | DISCUSSION

New technology in nucleic acid-based detection has started to take the place of conventional assays that are laborious, time-consuming, and limited applied to POC diagnosis. CRISPR (regularly interspaced short palindromic repeats) and Cas enzyme (CRISPR-associated) are bacteria and archaea's defense system that protects organisms from invading viruses.[36,37] Biotechnology based on CRISPR is not only applied in gene editing for biology engineering but has also been developed as an effective tool for molecular diagnosis. Recent studies showed that RNA-guided CRISPR/Cas nuclease-based assay successfully detects nucleic acid targets, which can be developed as the next-generation diagnostic.[38,39]

As a recently emerged technology, CRISPR diagnostic has soon become a powerful tool for in vitro diagnostics and provides promising applications not only for pathogen detection but also for many other fields such as disease analysis.[40–43] The promising advantage of CRISPR-based diagnosis is of great suitability for the POC. However, only the CRISPR system is not sensitive enough to detect ultra-low amounts of nucleic acids. To further improve its sensitivity, a pre-amplification step is typically used ahead of the

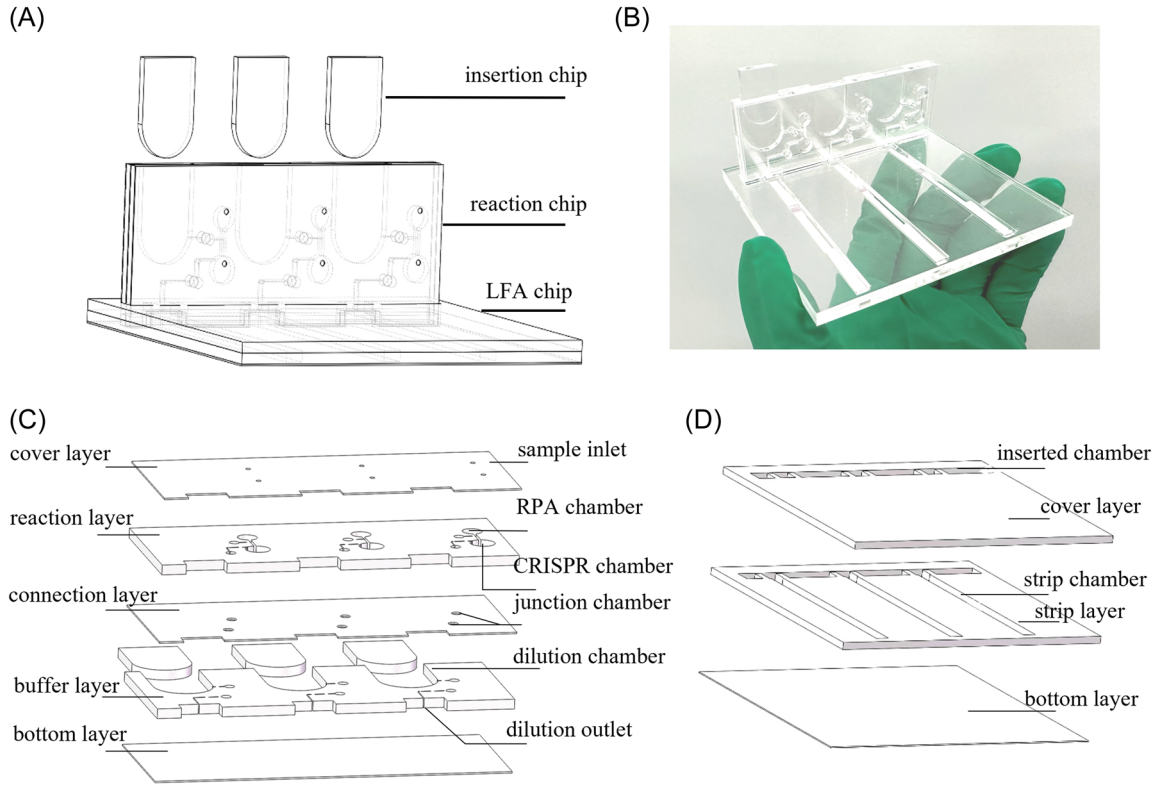

FIGURE 7 Schematic design of the manual microfluidic chip. (A) The exterior look of the manual microfluidic chip, including the insertion chip, reaction chip, and LFA chip. (B) Fabricated chip with lateral flow strips. (C) Details of the reaction chip. The chip contains five layers, with the cover, bottom, and connection layer 0.3 mm thick and the reaction chip, buffer layer 2 mm thick as well. Details of the main structure are shown. The reaction chip and buffer chip are connected by two junction chambers in the connection layer. (D) Details of LFA chip. The chip contains three layers, with a cover and strip layer of 2 mm thick and a bottom layer of 0.3 mm thick, respectively.

CRISPR reaction. RPA is a recently developed isothermal DNA amplification method with great advantages such as rapid, sensitive, and less requirement of sophisticated instruments, which also has been developed for pathogens detection.[28,44–46] Therefore, RPA combined with CRISPR has been applied to pathogen detection, especially in POC scenarios.[47]

As far as the standardized assays for detection of the respiratory tract pathogens, various methods such as qPCR, ELISA (Enzyme-Linked Immunosorbent Assay), CLIA (Chemiluminescence immunoassay), and LFIA (Lateral flow immunoassay) are widely used in practical use. However, some are considered time-consuming as qPCR and ELISA; and some have to be performed by specially trained personnel with sophisticated lab equipment in labs as qPCR and CLIA. In addition, lateral flow immunoassay is one of the most economical and simple methods, but the sensitivity of performance is not optimal as nucleic acid-based tests in practical use.[48] Each method can be applied in specific scenarios according to its characteristics (Table S2). Similarly, RPA is suitable for nucleic acid detection at the point of care because it is highly field-deployable and rapidly amplified within 15–20 min, and there is no requirement for complex instruments to maintain a temperature. Moreover, the lyophilization of isothermal amplification reagent is quite steady and could suffer ambient temperature which is an advantage for transportation.

In this study, we first present an assay that successfully detects SARS-CoV-2, influenza A, and influenza B based on RPA/CRISPR-Cas12a under a blue light illuminator system within 1 h and with a detection limit of 10^2 copies/μL. In clinical studies, the risk of transmission of COVID-19 decreases when the viral load drops below 1000 copies/μL. Additionally, the mean influenza virus load for hospitalized patients is above 5 log10 copies/mL, which indicates our current limit of detection is sufficient for virus screening.[49–51] More importantly, increasing test frequency is also an efficient strategy for breaking the pandemic as well as a fast turnaround time.[52]

Next, we combined the RPA/CRISPR-Cas12a method with lateral flow assay to achieve flexibility and simplicity. More importantly, a manually operated microfluidic chip with the lateral flow assay was used in this paper to satisfy POC utilization under various scenarios. Lab-on-chip (Microfluidics) is another novel technology that revolutionizes in vitro diagnostics. We utilized this advantage of microfluidics technology and designed this platform. This novel detection platform based on RPA/CRISPR-12a/LFA accomplishes three independent pathogen

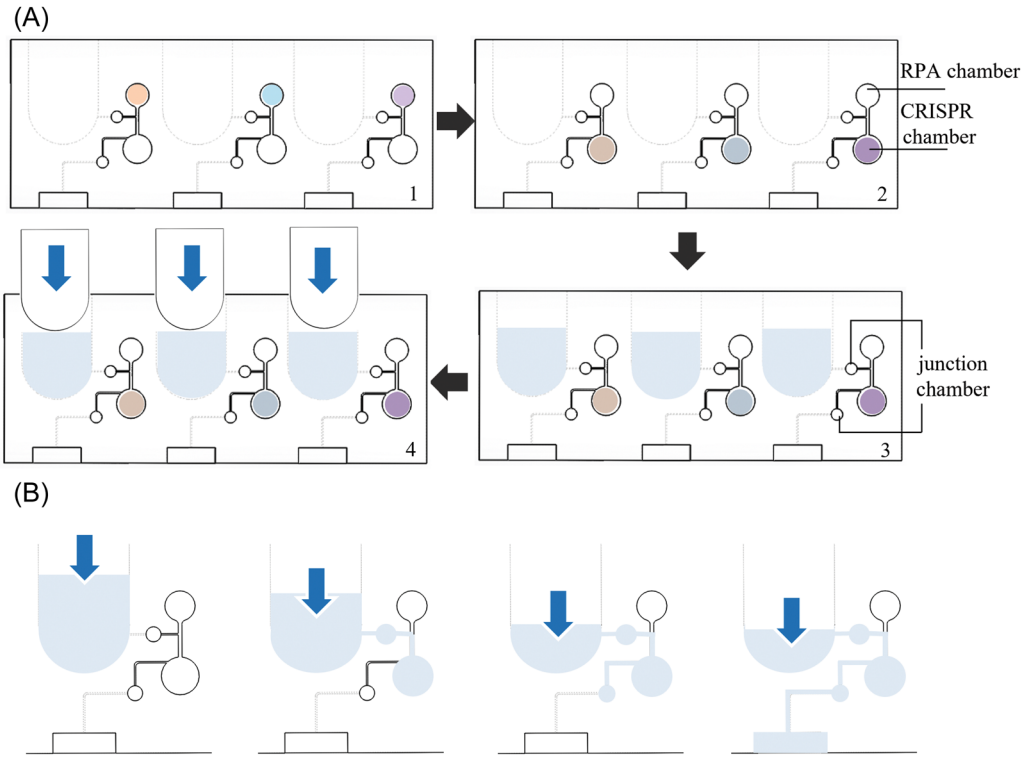

FIGURE 8 Schematic of fluid flow direction in the manual microfluidic chip. (A) Detailed steps in the reaction chip. 1, First RPA is taken in the RPA chamber; 2, RPA reaction flows into the CRSPR chamber; 3, Load the dilution buffer; 4, Insert the chip into the reaction chip. (B) Detail of fluid flow direction. The figure shows the flow direction of the dilution buffer after the insertion chip is inserted. RPA, recombinase polymerase amplification.

detections simultaneously and eliminates cross-contamination which provides an affordable way for diagnosis.

Furthermore, the panel of SARS-CoV-2 and influenza viruses was the first step in detecting the respiratory tract pathogens using our developed platform. Next, more critical pathogens will be detected based on this platform because this platform is very flexible and changeable for detection of various pathogens.

5 | CONCLUSIONS

In this study, a rapid and sensitive detection assay was developed for SARS-CoV-2 and influenza virus detection based on RPA combined with CRISPR-Cas12a with a detection limit of 10^2 copies/μL. A manual microfluidic chip was designed for RPA/CRPSIR-Cas12a coupled with lateral flow assay to achieve simplicity and flexibility for these three virus detections. The platform based on nucleic acid detection with optimized sensitivity and effectiveness will contribute to the detection of respiratory tract pathogens in different scenarios.

AUTHOR CONTRIBUTIONS

Yuning Wang, Liqiang Wu, Libo Nie, and Chungen Qian: participated in the study design. **Yuning Wang, Liqiang Wu, Ting Pan, Gang Wang, Tianxun Huang, and Zhentao Huang**: performed the experiments. **Yuning Wang and Xiaomei Yu**: designed and generated the microfluid chip. **Yuning Wang, Liqiang Wu, and Chungen Qian**: analyzed these results. **Yuning Wang**: wrote the manuscript. **Zhao Huang, Tianxun Huang, and Zhentao Huang**: participated in the interpretation and discussion. All authors reviewed and approved the manuscript.

ACKNOWLEDGEMENTS

The authors are grateful to Dr. Xiaohui Zhou (Southern University of Science and Technology, Shenzhen, China) for reading the manuscript and providing valuable suggestions.

CONFLICT OF INTEREST STATEMENT

The authors declare no conflicts of interest.

DATA AVAILABILITY STATEMENT

All data associated with this study are available in the main text. The data that supports the findings of this study are available in the supplementary material of this article.

ORCID

Yuning Wang http://orcid.org/0009-0008-6310-6837

REFERENCES

1. World Health Organization. The top 10 causes of death. 2020; https://www.who.int/en/news-room/fact-sheets/detail/the-top-10-causes-of-death
2. Langelier C, Kalantar KL, Moazed F, et al. Integrating host response and unbiased microbe detection for lower respiratory tract infection diagnosis in critically ill adults. *Proc Natl Acad Sci USA*. 2018;115(52):E12353-E12362.
3. de Steenhuijsen Piters WAA, Binkowska J, Bogaert D. Early life microbiota and respiratory tract infections. *Cell Host Microbe*. 2020;28(2):223-232.
4. Lim SS, Vos T, Flaxman AD, et al A comparative risk assessment of burden of disease and injury attributable to 67 risk factors and risk factor clusters in 21 regions, 1990-2010: a systematic analysis for the global burden of disease study 2010. *The Lancet*. 2012;380(9859):2224-2260.
5. Ferkol T, Schraufnagel D. The global burden of respiratory disease. *Ann Am Thorac Soc*. 2014;11(3):404-406.
6. Dasaraju PV, Liu C. Infections of the Respiratory System. In: Baron Sed. *Medical Microbiology*. 4th ed. Galveston (TX) 1996.
7. Hanada S, Pirzadeh M, Carver KY, Deng JC. Respiratory viral infection-induced microbiome alterations and secondary bacterial pneumonia. *Front Immunol*. 2018;9:2640.
8. Centers for Disease Control and Prevention website. Influenza (flu). Accessed September 23, 2023. https://www.cdc.gov/flu/about/burden/index.html
9. Centers for Disease Control and Prevention website. Influenza (Flu). 2023. Accessed September 23, 2023. https://www.cdc.gov/flu/about/burden/preliminary-in-season-estimates.htm
10. World Health Organization. Influenza (Seasonal). https://www.who.int/news-room/fact-sheets/detail/influenza-(seasonal), 2023.
11. Keilman LJ. Seasonal influenza (Flu). *Nurs Clin North Am*. 2019;54(2):227-243.
12. Zhu N, Zhang D, Wang W, et al. A novel coronavirus from patients with pneumonia in China, 2019. *N Engl J Med*. 2020;382(8):727-733.
13. Gorbalenya AE, Baker SC, Baric RS, et al, Coronaviridae Study Group of the International Committee on Taxonomy of V. The species severe acute respiratory syndrome-related coronavirus: classifying 2019-nCoV and naming it SARS-CoV-2. *Nat Microbiol*. 2020;5(4):536-544.
14. Dong E, Du H, Gardner L. An interactive web-based dashboard to track COVID-19 in real time. *Lancet Infect Dis*. 2020;20(5):533-534.
15. Fisher D, Heymann D. Q&A: the novel coronavirus outbreak causing COVID-19. *BMC Med*. 2020;18(1):57.
16. Guan W, Ni Z, Hu Y, et al. Clinical characteristics of coronavirus disease 2019 in China. *N Engl J Med*. 2020;382(18):1708-1720.
17. Huang C, Wang Y, Li X, et al. Clinical features of patients infected with 2019 novel coronavirus in Wuhan, China. *The Lancet*. 2020;395(10223):497-506.
18. Jackson CB, Farzan M, Chen B, Choe H. Mechanisms of SARS-CoV-2 entry into cells. *Nat Rev Mol Cell Biol*. 2022;23(1):3-20.
19. Dos Santos WG. Natural history of COVID-19 and current knowledge on treatment therapeutic options. *Biomed Pharmacother*. 2020;129:110493.
20. Harrison AG, Lin T, Wang P. Mechanisms of SARS-CoV-2 transmission and pathogenesis. *Trends Immunol*. 2020;41(12):1100-1115.
21. Ellis JE, Guest P, Lawson V, Loecherbach J, Lindner N, McCulloch A. Performance evaluation of the microfluidic antigen LumiraDx SARS-CoV-2 and flu A/B test in diagnosing COVID-19 and influenza in patients with respiratory symptoms. *Infect Dis Ther*. 2022;11(6):2099-2109.
22. Nypaver C, Dehlinger C, Carter C. Influenza and influenza vaccine: a review. *J Midwifery Womens Health*. 2021;66(1):45-53.
23. Dao TL, Hoang VT, Colson P, Million M, Gautret P. Co-infection of SARS-CoV-2 and influenza viruses: a systematic review and meta-analysis. *J Clin Virol*. 2021;1(3):100036.
24. Houser K, Subbarao K. Influenza vaccines: challenges and solutions. *Cell Host Microbe*. 2015;17(3):295-300.
25. Lim YW, Steinhoff M, Girosi F, et al. Reducing the global burden of acute lower respiratory infections in children: the contribution of new diagnostics. *Nature*. 2006;444(suppl 1):9-18.
26. Arizti-Sanz J, Bradley A, Zhang YB, et al. Simplified Cas13-based assays for the fast identification of SARS-CoV-2 and its variants. *Nat Biomed Eng*. 2022;6(8):932-943.
27. Böger B, Fachi MM, Vilhena RO, Cobre AF, Tonin FS, Pontarolo R. Systematic review with meta-analysis of the accuracy of diagnostic tests for COVID-19. *Am J Infect Control*. 2021;49(1):21-29.
28. Piepenburg O, Williams CH, Stemple DL, Armes NA. DNA detection using recombination proteins. *PLoS Biol*. 2006;4(7):e204.
29. Feng W, Peng H, Xu J, et al. Integrating reverse transcription recombinase polymerase amplification with CRISPR technology for the One-Tube assay of RNA. *Anal Chem*. 2021;93(37):12808-12816.
30. Lobato IM, O'Sullivan CK. Recombinase polymerase amplification: basics, applications and recent advances. *TrAC Trends Anal Chem*. 2018;98:19-35.
31. Qian J, Boswell SA, Chidley C, et al. An enhanced isothermal amplification assay for viral detection. *Nat Commun*. 2020;11(1):5920.
32. Park M, Won J, Choi BY, Lee CJ. Optimization of primer sets and detection protocols for SARS-CoV-2 of coronavirus disease 2019 (COVID-19) using PCR and real-time PCR. *Exp Mol Med*. 2020;52(6):963-977.
33. Shu B, Kirby MK, Davis WG, et al. Multiplex real-time reverse transcription PCR for influenza A virus, influenza B virus, and severe acute respiratory syndrome coronavirus 2. *Emerging Infect Dis*. 2021;27(7):1821-1830.
34. Sharma N, Hoshika S, Hutter D, Bradley KM, Benner SA. Recombinase-based isothermal amplification of nucleic acids with self-avoiding molecular recognition systems (SAMRS). *ChemBioChem*. 2014;15(15):2268-2274.
35. Thomas M, Bomar PA Upper Respiratory Tract Infection. In: *StatPearls*. Treasure Island (FL) 2023.
36. Wiedenheft B, Sternberg SH, Doudna JA. RNA-guided genetic silencing systems in bacteria and archaea. *Nature*. 2012;482(7385):331-338.
37. Jinek M, Chylinski K, Fonfara I, Hauer M, Doudna JA, Charpentier E. A programmable dual-RNA-guided DNA endonuclease in adaptive bacterial immunity. *Science*. 2012;337(6096):816-821.
38. Chertow DS. Next-generation diagnostics with CRISPR. *Science*. 2018;360(6387):381-382.
39. Li Y, Li S, Wang J, Liu G. CRISPR/Cas systems towards next-generation biosensing. *Trends Biotechnol*. 2019;37(7):730-743.
40. Liang M, Li Z, Wang W, et al. A CRISPR-Cas12a-derived biosensing platform for the highly sensitive detection of diverse small molecules. *Nat Commun*. 2019;10(1):3672.
41. Chen W, Luo H, Zeng L, et al. A suite of PCR-LwCas13a assays for detection and genotyping of Treponema pallidum in clinical samples. *Nat Commun*. 2022;13(1):4671.
42. Weisheit I, Kroeger JA, Malik R, et al. Simple and reliable detection of CRISPR-induced on-target effects by qgPCR and SNP genotyping. *Nat Protoc*. 2021;16(3):1714-1739.
43. Gootenberg JS, Abudayyeh OO, Kellner MJ, Joung J, Collins JJ, Zhang F. Multiplexed and portable nucleic acid detection platform with Cas13, Cas12a, and Csm6. *Science*. 2018;360(6387):439-444.
44. Rohrman BA, Richards-Kortum RR. A paper and plastic device for performing recombinase polymerase amplification of HIV DNA. *Lab Chip*. 2012;12(17):3082-3088.
45. Abd El Wahed A, El-Deeb A, El-Tholoth M, et al. A portable reverse transcription recombinase polymerase amplification assay for rapid detection of foot-and-mouth disease virus. *PLoS One*. 2013;8(8):e71642.

46. Boyle DS, McNerney R, Teng Low H, et al. Rapid detection of Mycobacterium tuberculosis by recombinase polymerase amplification. *PLoS One*. 2014;9(8):e103091.
47. Gootenberg JS, Abudayyeh OO, Lee JW, et al. Nucleic acid detection with CRISPR-Cas13a/C2c2. *Science*. 2017;356(6336):438-442.
48. Dinc HO, Karabulut N, Alacam S, et al Evaluation of the diagnostic performance of a SARS-CoV-2 and influenza A/B combo rapid antigen test in respiratory samples. *Diagnostics (Basel)*. 2023;13(5):972.
49. La Scola B, Le Bideau M, Andreani J, et al. Viral RNA load as determined by cell culture as a management tool for discharge of SARS-CoV-2 patients from infectious disease wards. *Eur J Clin Microbiol Infect Dis*. 2020;39(6):1059-1061.
50. Wölfel R, Corman VM, Guggemos W, et al. Virological assessment of hospitalized patients with COVID-2019. *Nature*. 2020;581(7809):465-469.
51. Granados A, Peci A, McGeer A, Gubbay JB. Influenza and rhinovirus viral load and disease severity in upper respiratory tract infections. *J Clin Virol*. 2017;86:14-19.
52. Larremore DB, Wilder B, Lester E, et al. Test sensitivity is secondary to frequency and turnaround time for COVID-19 screening. *Sci Adv*. 2021;7(1):eabd5393.

SUPPORTING INFORMATION

Additional supporting information can be found online in the Supporting Information section at the end of this article.

How to cite this article: Wang Y, Wu L, Yu X, et al. Development of a rapid, sensitive detection method for SARS-CoV-2 and influenza virus based on recombinase polymerase amplification combined with CRISPR-Cas12a assay. *J Med Virol*. 2023;95:e29215. doi:10.1002/jmv.29215